

SKA1-mid VLBIによる 近傍AGNトーラスのゼーマン測定

澤田-佐藤聡子, 工藤祐己, 赤堀卓也

2018年7月22日 SKA時代のVLBIサイエンス@国立天文台三鷹

AGN 領域の磁場の重要性

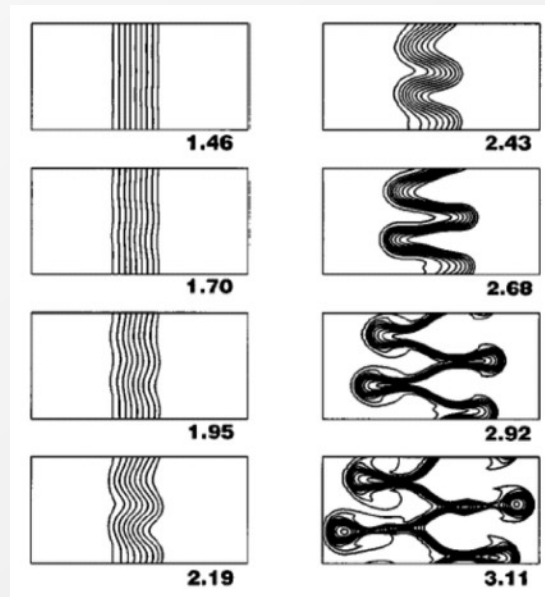
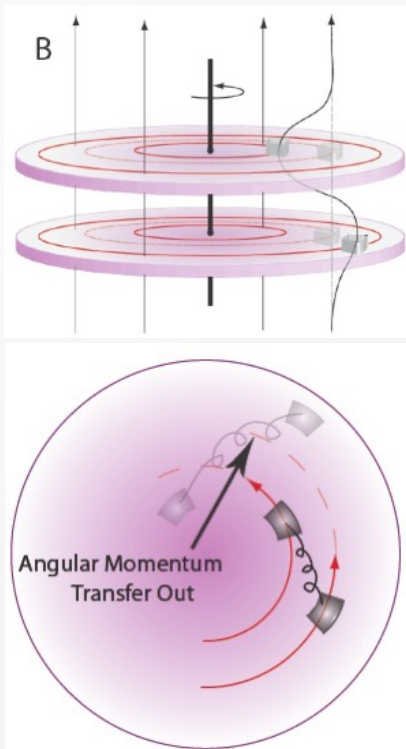
- ジェット駆動の説明 → 秦さんの講演
- 質量降着、角運動量損失の説明

AGNの活動性に
磁場が大いに関わる

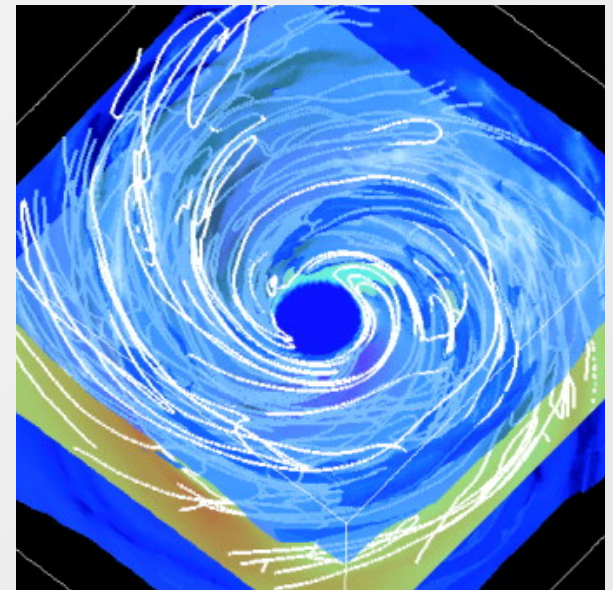
磁気回転不安定性 (MRI)

Balbus & Hawley 1991

トーラス内の磁力線がMRIにより進化



Balbus & Hawley 1998



Machida & Matsumoto 2003

AGNトーラス

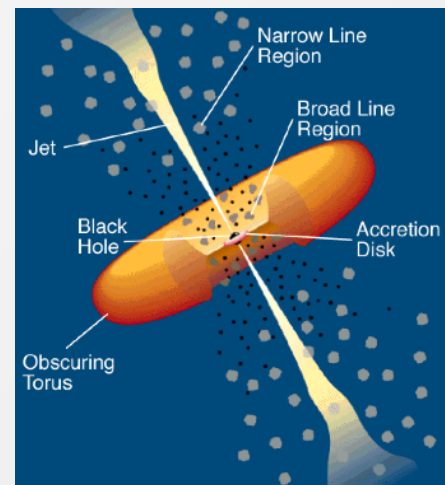
■ AGN統一モデル Antonucci, 1993

- 中心にブラックホール
- その周囲に降着円盤
- その周囲にトーラス
 - 典型的に $<10\text{pc}$ のサイズ

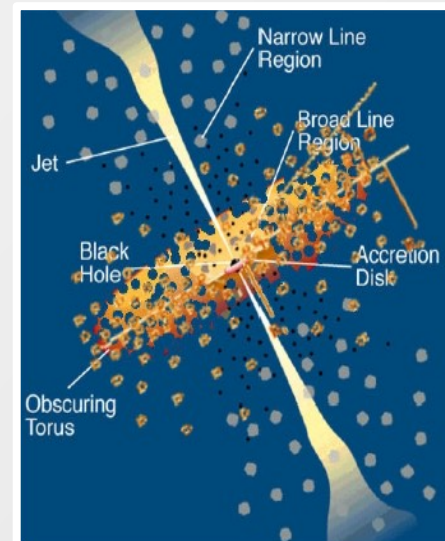
■ Clumpyトーラス Nenkova+, 2002, 2008

- 非一様密度分布、小さなガス塊
- トーラスの厚みの速度分散を説明

撮像観測には $<10\text{pc}$ を見分ける角分解能が必要
ガス塊を分解するなら $<1\text{pc}$



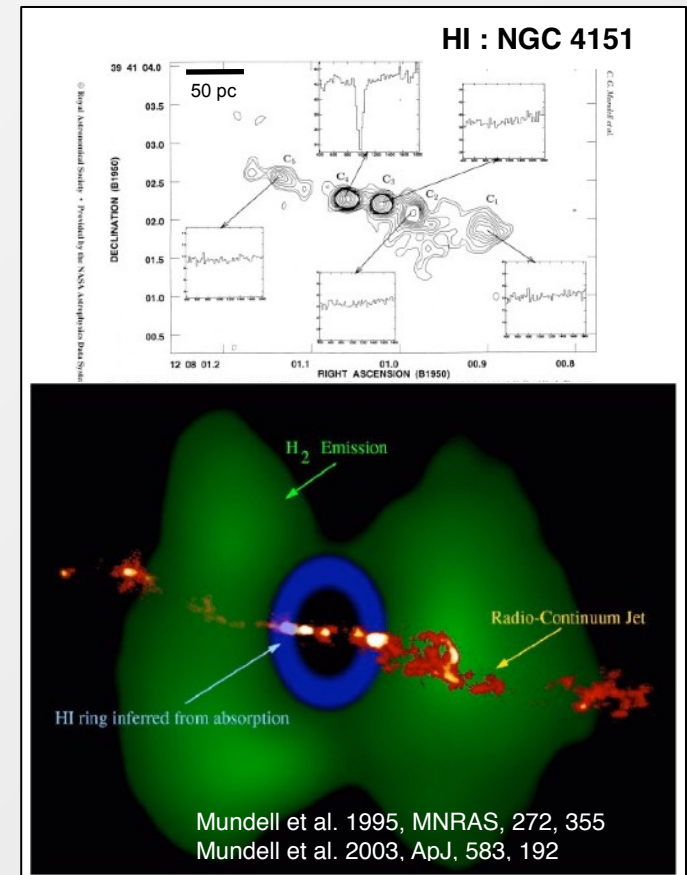
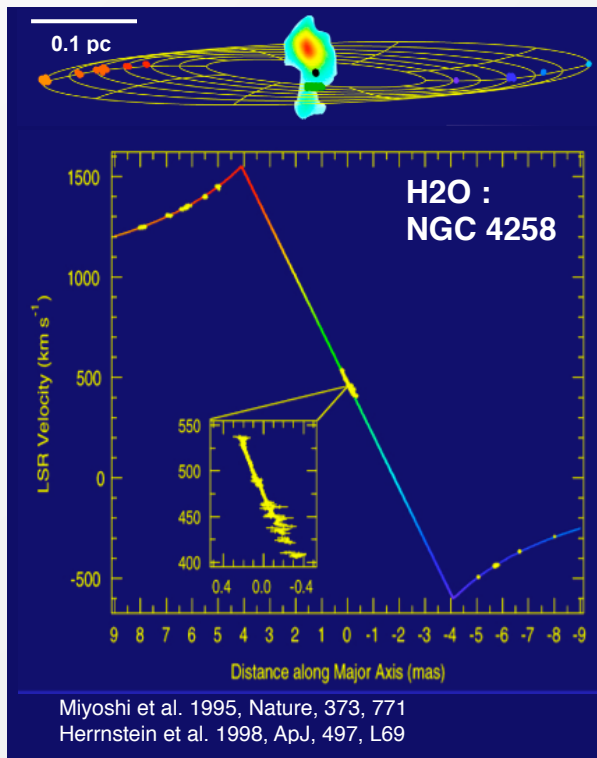
Urry & Padovani, 1995



Ramos Almeida+, 2011

AGNトーラスとVLBI

- 近傍AGN (~10Mpc)のトーラスを分解
 - H2Oメガメーザー
 - 中性水素(HI)吸収線, OH吸収線



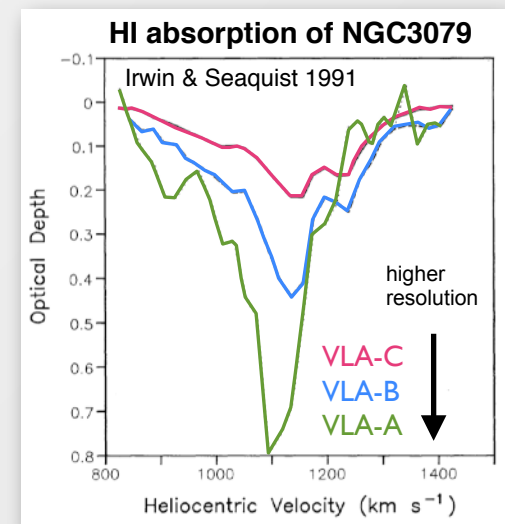
吸収線とVLBI

■ Thermal lines とVLBI

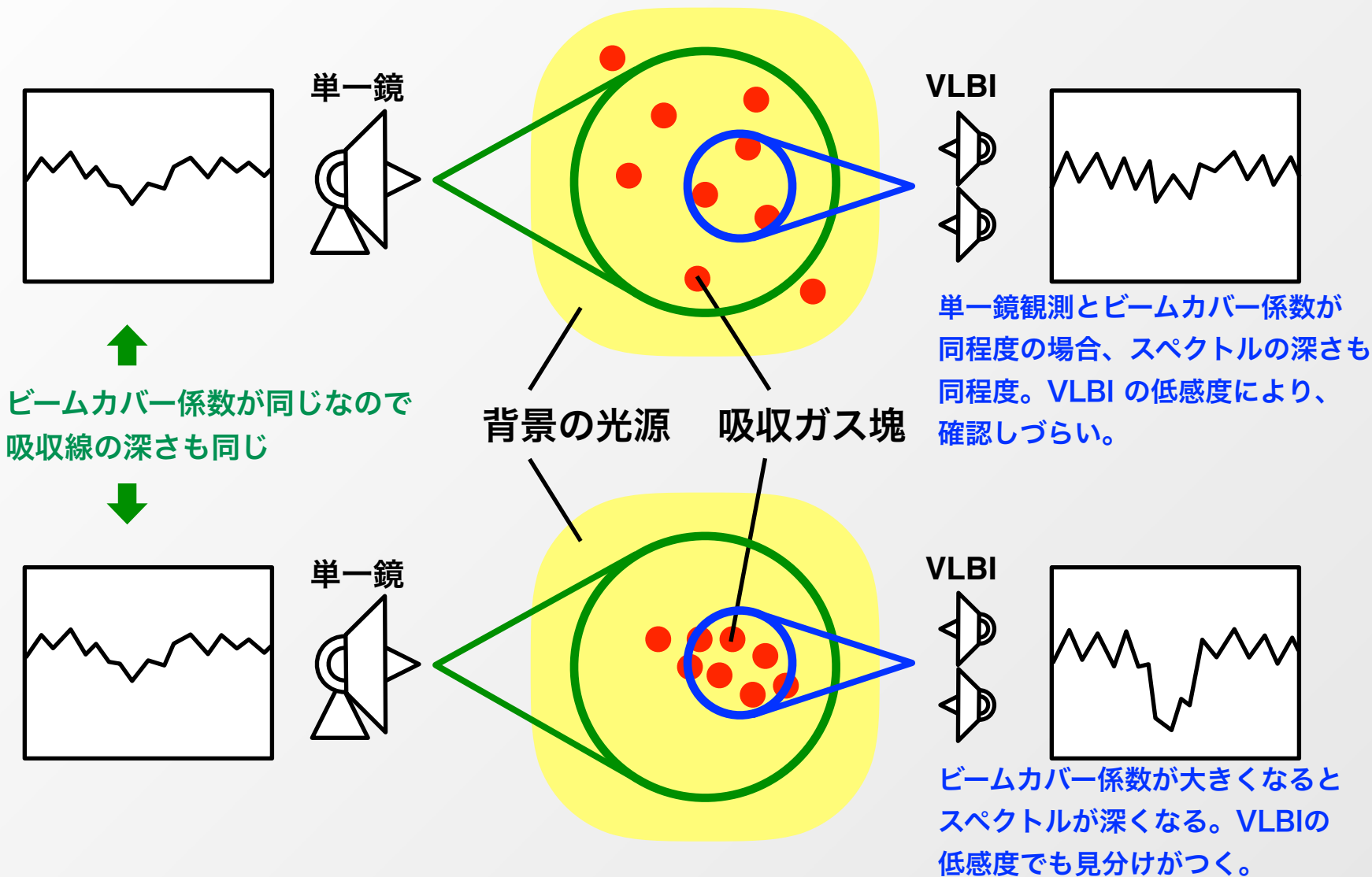
- 系外銀河中心部によく付随、良いプローブ
- 輝線は現在のVLBIでは検出不可
- シンクロトロン放射を背景とする吸収線ならVLBIで検出可

■ コンパクトな吸収ガスとVLBI

- 吸収ガスがコンパクトな時、細いビームが検出に有利
ビームカバー係数が大きくなるため



ビームカバー係数 Beam covering factor



過去のVLBI観測の例

■ HCN J=1-0 (88.631GHz) 吸収線@NGC1052

■ IRAM干渉計PdBI (100pc) Liszt & Lucas 2004

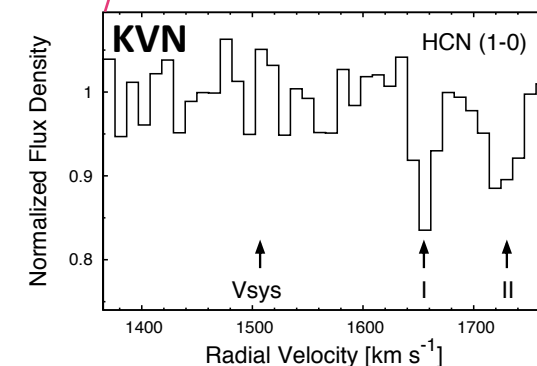
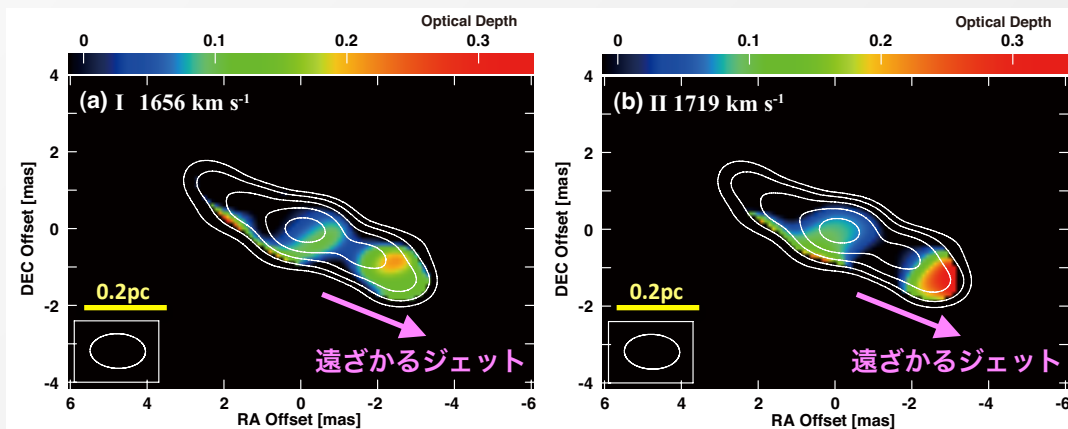
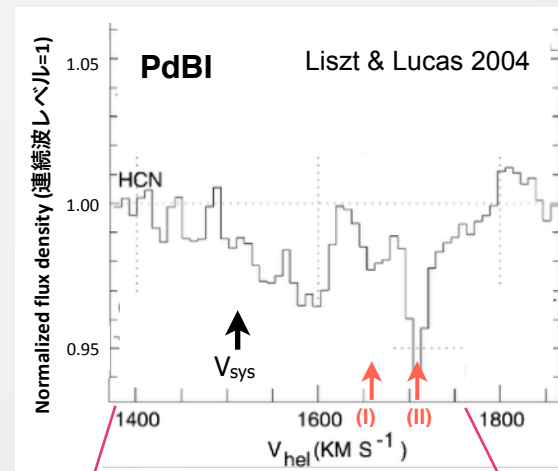
■ 連続波レベルより -0.05

■ KVN (0.1pc) Sawada-Satoh+ 2016

■ I, II成分: -0.15

■ V_{sys} 成分: -0.05 (雑音レベル)

I, II成分でビームカバー係数が上昇



Sawada-Satoh+ (2016)

過去のVLBI観測の例(続)

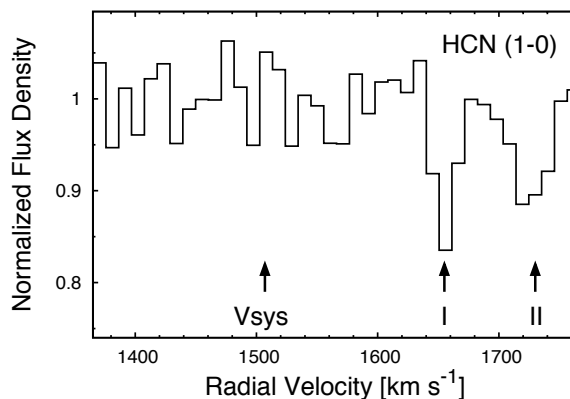
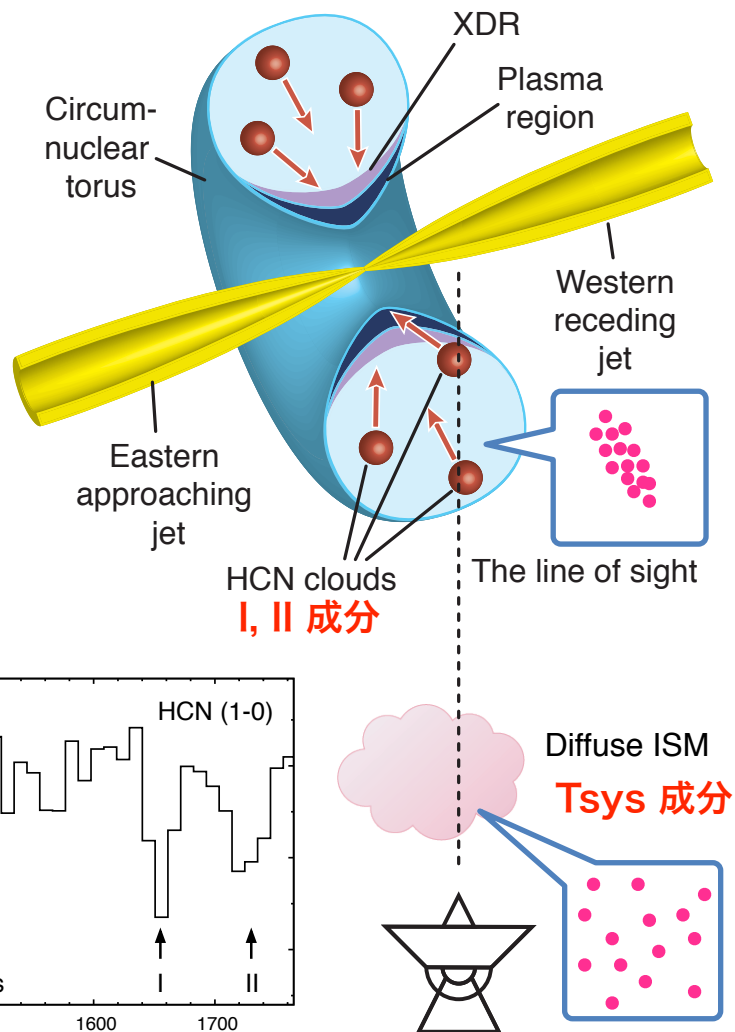
■ VLBIの利点

- トーラスの向きやサイズを判別
- 熱的放射は検出しない
- Diffuse ISM の吸収線は雑音に埋まる。ビームカバー係数に変化なし。
- コンパクトなガス塊の吸収線はビームカバー係数が大きくなり検出しやすくなる

AGN領域のコンパクトなガス
(例:トーラス)のみ検出する

NGC1052トーラスの描像

Sawada-Sato+ 2016



Diffuse ISM
Ts_{sys} 成分

系外銀河中心の HI 吸収線

- HI: SKA の主要な観測対象
- CSO/GPSのほぼ半数
- 他のAGNでも
- スターバーストでも
- VLBI画像37例(2010年時点)
 - 半数がAGN disk/torus
 - 南天も数例
 - まだ分解能不足

TABLE 4
HI Observations of AGNs and Starbursts at High Angular Resolution^a

Galaxy	HI Detection ^b	Line Profile ^c	HI Location ^d	Ref.
<i>1. Compact symmetric objects</i>				
4C 31.04, B0116+319, J0119+3210	Both lobes	N, B, M	AGN torus + infalling HVC	1
4C 37.11, B0402+379, J0405+3803	One lobe	B, M	AGN torus	2
OQ +122, PKS 1413+135, J1415+1320	One lobe	N	GMC in kpc disk	3
B1934-638, PKS 1934-63, J1939-6342	...	N	Infalling HVC?	4
B1946+708, J1945+7055	Both lobes	N, B, M	AGN torus	5,6
B2352+495, J2355+4950	One lobe	N, B, M	AGN disk + infalling cloud	This work
<i>2. Non-CSO radio sources: double jet/lobe systems as imaged by VLBI</i>				
3C 49, B0138+136, J0141+1353	One lobe	N, M	Cloud/jet interaction	7
NGC 1052, B0238-084, J0241-0815	Both radio jets	N, M	Nuclear and/or galactic?	8
Mik 6, IRAS 06457+7429, J0652+7425	One side of jet	N	kpc disk	9
Hydra A, 3C 218, B0915-118, J0918-1205	Both jets+core	N, M	AGN disk	10
3C 236, B1003+351, J1006+3454	One lobe	B	Cloud/jet interaction	1
NGC 3894, B1146+596, J1148+5924	Lobes + core	N, M	AGN torus	11
3C 268.3, B1203+6430, J1206+6413	One lobe	N	Cloud/jet interaction	7
NGC 4151, B1208+396, J1210+394	One radio jet	N, M	AGN torus	12
NGC 4261, B1216+061, J1219+0549	Counterjet+core?	N, M?	AGN disk	13
Mik 231, IRAS 12540+5708, J1256+5652	Diffuse cont.	B	~100 pc disk	14
4C 12.50, IRAS 13451+1232, J1347+1217 ^e	Counterjet	B, M	Cloud/jet interaction	15
3C 293, B1350+3141, J1352+3126	Both jets+core	B, N, M	Outer (8 kpc) and ~400 pc disk	16
NGC 5793, IRAS 14566-1629, J1459-1641	Both lobes	N, M	~1 kpc torus?	17
NGC 5929, B1524+4151, J1526+4140	One lobe	N	AGN ring, or bar?	18
PKS 1814-63, J1820-6343	Both lobes	M, N	AGN disk + Cloud/jet interaction?	19
IC 5063, B2048-572, J2052-5704	One lobe	B, M	Cloud/jet interaction	20
TXS 2226-184, IRAS 22265-1826, J2229-1810	Radio jet	B	Nuclear region, cloud/jet interaction?	21
NGC 7469, B2300+0836, J2303+0852	Radio core	N	Nuclear or galactic?	22
PKS 2322-123, J2325-1207	One jet + core	B, M	AGN disk + infall?	23
NGC 7674, IRAS 23254+0830, J2327+0846	One lobe + core?	B, N, M	AGN disk/torus	24
<i>3. Non-CSO radio sources: single jet + core systems as imaged by VLBI</i>				
NGC 315, B0055+300, J0057+3021	One jet + core	N	Infalling cloud	25
NGC 3079, IRAS 09585+5555, J1001+5540	One jet + core	N, M	AGN torus	26
Cen A, NGC 5128, B1322-428, J1325-4301	One jet	N, M	kpc disk or rings	25
PKS 1549-79, B1549-790, J1557-7913	One jet + core	N	Nuclear region?	27
Cygnus A, IRAS 19577+4035, J1959+4044	Counterjet + core?	B	Torus or 2 kpc ring	1
DA 529, B2050+364, J2052+3635	One jet + core	N, M	NLR/BLG (<1 kpc)	28
<i>4. Non-CSO radio sources: starbursts</i>				
NGC 2146, 4C+78.06, B06106+7822, J0618+7821	Starburst cont.	B, N, M	Disk or ring	29
IC 694, Arp 299, Mrk 171, B1125+588, J1128+5834	Starburst cont.	...	250 pc disk	30
Mik 273, B1342+5608, J1344+5553	Starburst cont.	B, M	Starburst cores	31
Arp 220, B1532+2339, J1534+2330	Starburst cont.	N, B, M	Disks in starburst cores	32
PGC 060189, IRAS 17208-0014, J1723-0016	Starburst cont.	B, N, M	Nuclear ~1 kpc	33

Notes.

^a Interferometric observations with baselines greater than 100 km. The sources are divided in four groups: CSOs, non-CSO radio sources with detection of two radio jets or lobes in opposite sides of a central core, non-CSO radio sources dominated by core-jet emission (although a weak counterjet may be detected, e.g., Cygnus A; Conway 1999), and starburst galaxies. ^b Indicates whether HI absorption was detected toward all radio continuum emission (both lobes and core, or starburst), or only toward one radio lobe. ^c Detection of broad lines ($\Delta V > 100 \text{ km s}^{-1}$) is indicated with "B," narrow lines ($\Delta V < 100 \text{ km s}^{-1}$) with "N," multiple lines in the spectrum (overlapped or otherwise) with "M." ^d Most likely (or at least preferred), location of the HI material with respect to the AGN as discussed in the reference paper, e.g., associated with a disk of torus within ~100 pc from the AGN, with GMCs or HVCs at galactic (kiloparsec) scales. ^e The HI distribution in this source has not been imaged with VLBI; however, the absorption is against the compact radio continuum given detection of HI with three LBA baselines (Véron-Cetty et al. 2000; see also Section 1.1). ^f The classification of 4C+12.50 is controversial, see Section 1.1.

References. (1) Conway 1999; (2) Rodríguez et al. 2009; (3) Perlman et al. 2002; (4) Véron-Cetty et al. 2000; (5) Peck et al. 1999; (6) Peck & Taylor (2001); (7) Lahaie et al. 2006; (8) Vermeulen et al. 2003a; (9) Gallimore et al. 1998; (10) Taylor 1996; (11) Peck & Taylor 1998; (12) Mundell et al. 2003; (13) van Langevelde et al. 2000; (14) Carilli et al. 1998; (15) Morganti et al. 2004; (16) Beswick et al. 2004; (17) Pihlström et al. 1999; (18) Cole et al. 1998; (19) Morganti et al. 2000; (20) Oosterloo et al. 2000; (21) Taylor et al. 2004; (22) Beswick et al. 2002; (23) Taylor et al. 2002; (24) Momjian et al. 2003a; (25) Peck 1999; see also Morganti 2004; (26) Sawada-Satoh et al. 2000; (27) Holt et al. 2006; (28) Vermeulen et al. 2006; (29) Turchi et al. 2004; (30) Polatidis & Aalto 2001; (31) Carilli & Taylor 2000; (32) Mundell et al. 2001; (33) Momjian et al. 2003b.

過去の高分解能ゼーマン測定@系外銀河中心

- HI 吸収線@NGC1275 (セイファートAGN) Sarma+ 2005
 - VLA (1.5秒角, 700pc) トーラスよりずっと大きいサイズ
 - $B_{\text{los}} = 21.5 \text{ microG}$

THE ASTRONOMICAL JOURNAL, 130:2566–2570, 2005 December
© 2005. The American Astronomical Society. All rights reserved. Printed in U.S.A.

VERY LARGE ARRAY H I ZEEMAN OBSERVATIONS OF NGC 1275 (PERSEUS A)

A. P. SARMA,¹ E. MOMJIAN,² T. H. TROLAND,³ AND R. M. CRUTCHER⁴

Received 2005 April 5; accepted 2005 August 30

ABSTRACT

We present Very Large Array (VLA) observations of 21 cm H I absorption in the high-velocity (HV) system toward the external galaxy NGC 1275 (Per A). The primary motivation for our observations is to examine whether the only existing (single-dish) detection of the magnetic field in an external galaxy will stand up to independent scrutiny with an interferometer. The H I absorption profile in the HV system toward NGC 1275 has a number of velocity components. In this paper, we focus on the prominent narrow component at 8114 km s^{-1} , in which we have detected the Zeeman effect. The measured line-of-sight magnetic field is $B_{\text{los}} = -21.5 \pm 6.5 \mu\text{G}$. Within the errors, this is consistent with the single-dish detection. A weighted average of the single-dish and VLA detections gives a value for the line-of-sight magnetic field of $B_{\text{los}} = -10.7 \pm 3.2 \mu\text{G}$. The derived ratio of total internal kinetic energy to gravitational energy suggests that the clouds responsible for H I absorption are likely not gravitationally bound. The ratio of magnetic energy to total internal kinetic energy indicates that magnetic effects are likely dominant in these clouds. Finally, the measured ratio of mass to magnetic flux is found to be much lower than the critical value, indicating that the observed H I absorbing clouds are significantly subcritical. This agrees with a recent study of H I absorbing clouds in the cold neutral medium of our Galaxy, thereby extending an important result for Galactic clouds to an extragalactic case.

Key words: galaxies: active — galaxies: individual (NGC 1275) — galaxies: ISM — galaxies: magnetic fields — radio lines: galaxies

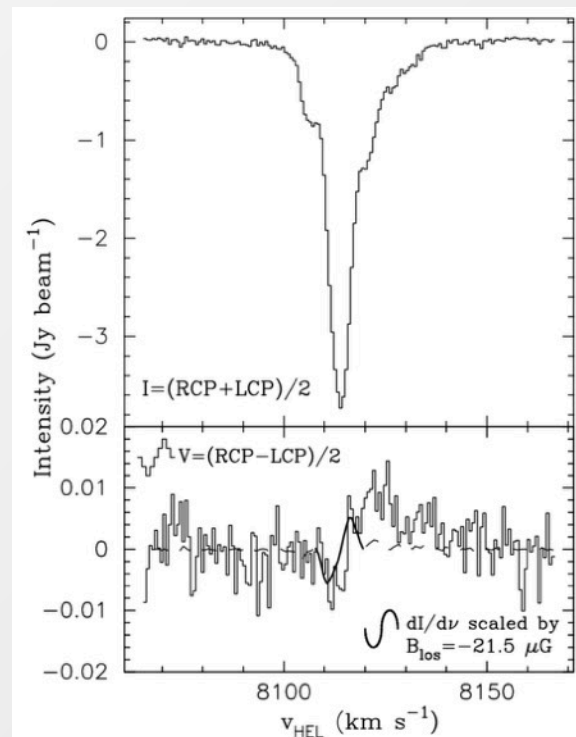


FIG. 3.—Stokes I (top) and V (bottom) profiles of the 21 cm H I absorption in the HV system toward NGC 1275. The superposed curve in the bottom panel shows the derivative of I scaled by $B_{\text{los}} = -21.5 \mu\text{G}$. The continuous portion of this curve shows the channels over which the fit was made.

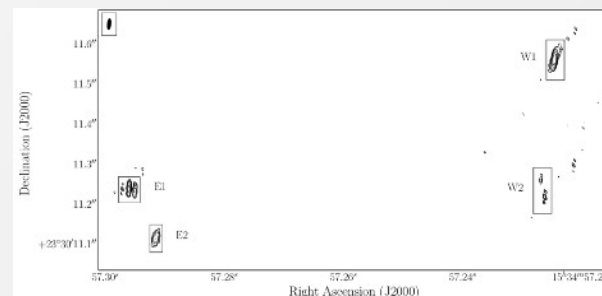
過去の高分解能ゼーマン測定@系外銀河中心

■ OHメガメーザー@Arp220 (スターバースト) McBride+ 2014

■ VLBI (20mas, 10pc)

■ $B_{\text{los}} = 1\sim 5 \text{ mG}$

初のパーセクスケール測定
ただし、トーラスではない



Parsec-scale magnetic fields in Arp 220

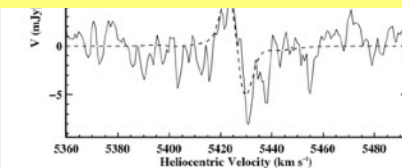
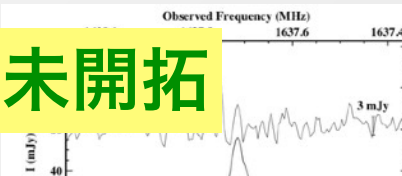
James
Monthly
ras/stu

Published: 19 December 2014 Article history ▾

AGNごく近傍のゼーマン測定はまだ未開拓

AGNトーラスの回転向きと磁場の向き
の関係すら
まだまだ未説明

direction as features at the same velocity identified in previous Zeeman observations with Arecibo alone. The agreement between single dish and VLBI results provides critical validation of previous Zeeman splitting observations of OH megamasers that used a single large dish. The measured magnetic field strengths indicate that magnetic energy densities are comparable to gravitational energy in OH maser clouds. We also compare our total intensity results to previously published VLBI observations of OH megamasers in Arp 220. We find evidence for changes in both structure and amplitude of the OH maser lines that are most easily explained by variability intrinsic to the masing region, rather than variability produced by interstellar scintillation. Our results demonstrate the potential for using high-sensitivity VLBI to study magnetic fields on small spatial scales in extragalactic systems.



(b) Stokes I and V for the OH maser spot at E1.1 ($15^{\text{h}}34^{\text{m}}57^{\text{s}}.295$, $+23^{\circ}30'11.235''$).

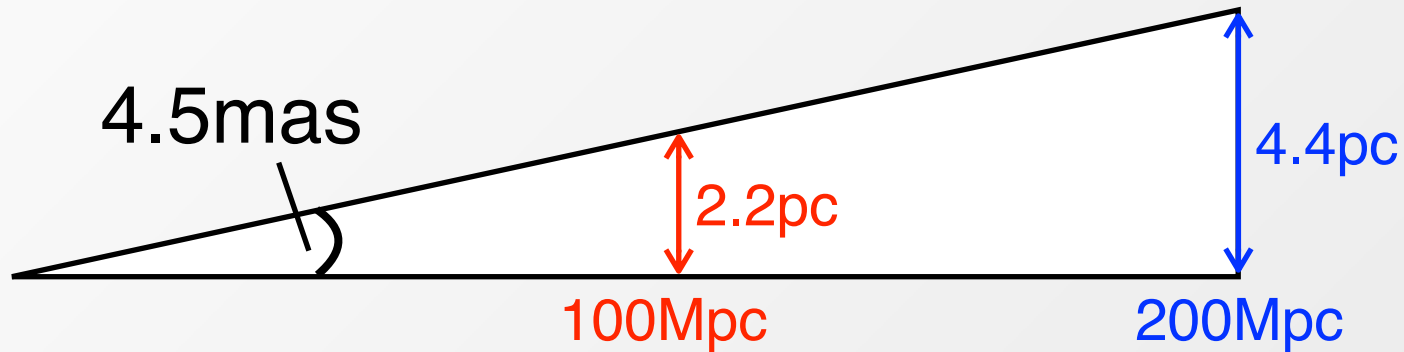
SKA1-mid で VLBI

- SKA1-mid スペック@L-band
 - SKA-Japan WS 2015 発表資料(赤堀さん)より
 - 感度: $A_{\text{eff}}/T_{\text{sys}}=1309 \Rightarrow \text{SEFD: } 2.1 \text{ Jy}$
 - SKA-VLBI 性能諸元でも SEFD: 5.5Jy
 - 周波数分解能: 3.9kHz
- 周波数分解能 : HI のゼーマン分裂 2.8 Hz/microG
 - 周波数分解能の数チャンネル分ずれると判別可能
 - 5mGなら14kHzのずれ。3.6チャンネル分。
 - 3.9kHzの連続波 channel map が有意に描ければ、5mGが検出可能

SKA1-mid で VLBI

■ 角分解能：南半球の望遠鏡間で VLBI

■ 例：豪Parkesとの基線長 9700 km → 4.5mas@1.4GHz



近傍 AGN ($\sim 200\text{Mpc}$) なら、トーラスの分解は可能

SKA1-mid で VLBI

- 感度：南半球の1.4GHz受信機を持つ望遠鏡間で VLBI

$$\langle \text{SEFD} \rangle = \frac{1}{\sqrt{\sum_{i,j=1}^{n; i < j} \frac{1}{\text{SEFD}_i \text{SEFD}_j}}}$$

	直径[m]	SEFD[Jy]
Narrabri	22	340
Mopra	22	340
Parkes	64	40
Hobart	26	470
Phased SKA		2.1

http://www.atnf.csiro.au/vlbi/documentation/vlbi_antennas/index.html

この観測網

$$\langle \text{SEFD} \rangle = 7.7 \text{ [Jy]}$$

$$\Delta I = \frac{\langle \text{SEFD} \rangle}{\sqrt{\Delta \tau \Delta \nu}}$$

$\Delta \tau$: integration time
(5 hr)

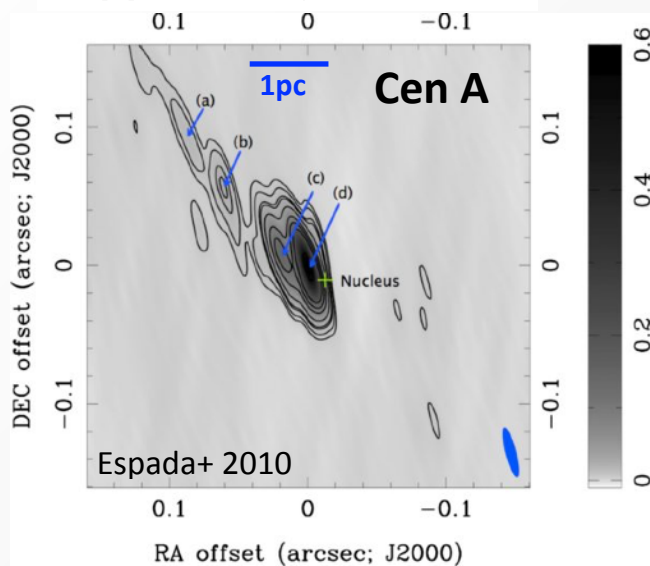
$\Delta \nu$: frequency resolution
(3.9 kHz)

$$\therefore \Delta I = 1.044 \text{ [mJy beam}^{-1}\text{]}$$

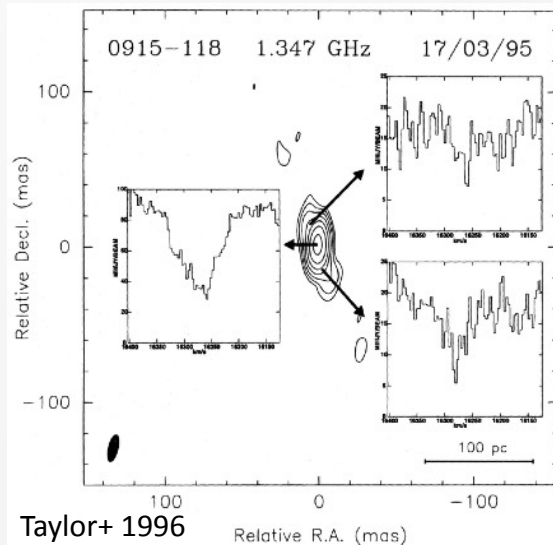
**AGN コア/ジェットのフラックス密度
5mJy以上あれば5 σ で検出可能**

観測ターゲットの例 ~ 前述の VLBI 37例より

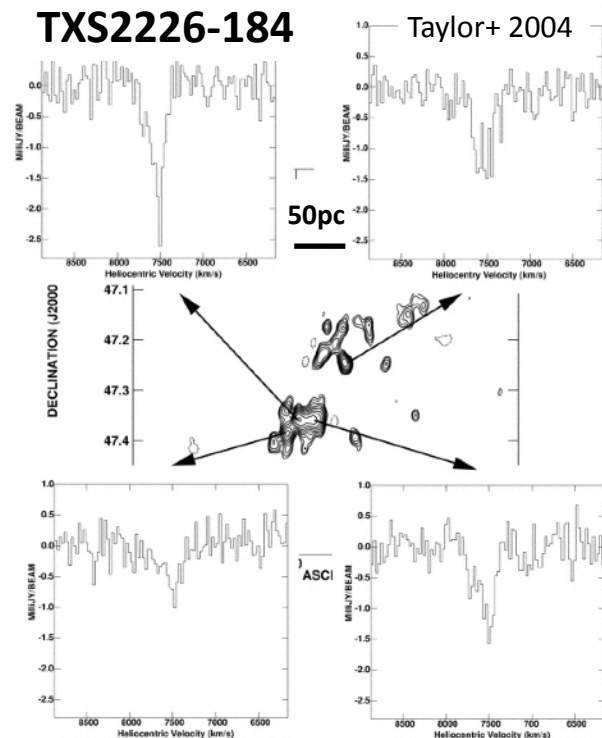
一番近くの明るい天体



200Mpcより遠い天体



かなり暗めの天体



Source	Distance [Mpc]	Linear scale for 4.5mas [pc]	Peak I @1.4GHz [mJy/beam]
Cen A	3.8	0.08	600
0915-118	240	5.3	40
TXS2226-184	102	2.2	10

<10pc

>5mJy/beam

前述の37例ならば
ゼーマン測定できそう

まとめ

- AGN 領域の活動性に磁場は大きな役割
- 今後SKA-VLBIの高感度と高角分解能は
 - 近傍AGN トーラス/ディスク起源の吸収線 (HI, OH...)の検出を量産
 - 初のAGNトーラスのゼーマン測定実現可能
- SKA1-mid のスペックは本観測提案を十分推進可能
 - ただし1mGの検出なら**周波数分解能**は<1kHzが必要